

Calculating the Habitable Zone of Multiple Star Systems (<http://astro.twam.info/hz>)

Tobias W. A. Müller¹ and Nader Haghighipour^{1,2}

ABSTRACT

We have developed a comprehensive methodology and an interactive website for calculating the habitable zone (HZ) of multiple star systems. Using the concept of spectral weight factor, as introduced in our previous studies of the calculations of HZ in and around binary star systems, we calculate the contribution of each star (based on its spectral energy distribution) to the total flux received at the top of the atmosphere of an Earth-like planet, and use the models of the HZ of the Sun to determine the boundaries of the HZ in multiple star systems. Our interactive website for carrying out these calculations is publicly available at <http://astro.twam.info/hz>. We discuss the details of our methodology and present its application to some of the multiple star systems detected by the *Kepler* space telescope. We also present the instructions for using our interactive website, and demonstrate its capabilities by calculating the HZ for two interesting analytical solutions of the three-body problem.

Subject headings: Astrobiology: Habitable zone – Stars: Planetary systems – atmospheric effects

1. Introduction

It is widely accepted that stars form in clusters. Surveys of star-forming regions have indicated that approximately 70% of all stars in our galaxy are in binary or multiple star systems (Batten et al. 1989). An examination of 164 nearest G-dwarfs by Duquennoy & Mayor (1991), for instance, has shown that 62 of these stars are in binaries, 7 are in triplets, and 2 are members of two quadruple star systems. In the past few years, the *Kepler* space telescope has also detected many binary and multiple star systems. The *Kepler* Eclipsing Binary Catalog lists more than 2100 eclipsing binaries (Slawson et al. 2011) among which $\sim 20\%$ are within triple star systems.

¹Institute for Astronomy and Astrophysics, University of Tübingen, Auf der Morgenstelle 10, 72076 Tübingen, Germany

²Institute for Astronomy and NASA Astrobiology Institute, University of Hawaii-Manoa, Honolulu, HI 96822, USA

A survey of the currently known planet-hosting stars indicates that slightly more than 8% of these stars have stellar companions (Rein 2012). While the majority of these stars are in binaries, some are also in triple and quadruple systems. For instance, Kepler 64, which has a binary stellar companion and is host to a circumbinary planet (Schwamb et al. 2013), is in fact a member of a quadruple stellar system. The M star Gliese 667 (Anglada-Escudé et al. 2012; Delfosse et al. 2013), which is known to host at least seven planets, is part of a triple stellar system. The star 16 Cyg (Cochran et al. 1997), the first multiple star system discovered to host a planet, consists of three stellar components.

The discovery of planets in multiple star systems has raised the question that whether such planetary systems can be habitable. As the habitability of a planet (and, therefore, the system’s HZ), in addition to the size, atmospheric composition, and orbital dynamics of the planet, depends also on the total flux received at the top of the planet’s atmosphere, the stellar multiplicity plays an important role in determining the range and location of the system’s HZ. Depending on their surface temperatures and orbital characteristics, each star of the system will have a different contribution to the total flux at the location of the planet. Within the context of binary stars during the past few years this topic has been addressed by Mason et al. (2013); Liu et al. (2013); Kane & Hinkel (2013); Eggl et al. (2013, 2012); Quarles et al. (2012).

Recently, Haghighipour & Kaltenegger (2013, hereafter, HK13) and Kaltenegger & Haghighipour (2013, hereafter, KH13) studied this concept within the context of binary star systems. These authors have shown that as the atmosphere of a planet interacts differently with the incident radiation from stars with different spectral energy distributions (SED), the contribution of each star of the binary to the total flux received by the planet will be different. In other words, considering the direct summation of the fluxes of the two stars as the total flux received at the top of the planet’s atmosphere, and using that quantity to calculate the total insolation on the planet’s surface will not be a correct approach and will result in an inaccurate value for the planet’s equilibrium temperature. The fact that the planet’s atmosphere responds differently to stellar radiations with different incident energy indicates that the contribution of each star to the total flux received at the top of the planet’s atmosphere has to be weighted according to the star’s SED. As shown by HK13 and KH13, such a weight factor will be a function of the star’s effective temperature and will have different forms for different models of the Sun’s HZ. Considering the latest models of the habitability of Earth as presented by Kopparapu et al. (2013a,b), HK13 and KH13 derived a formula for the *spectral weight factor* of a star based on the star’s effective temperature, and presented an analytical formalism for calculating the HZ in S-type and P-type binary stars systems.

In this paper, we follow the same approach as presented by these authors and generalize their methodology to calculate the HZ in systems with $N \geq 2$ stars. Although in order to maintain stability, most multi-star systems have evolved into hierarchical configurations and have developed

large stellar separations (which depending on the effective temperatures of their stars may imply minimal contribution from one star in the extent of the HZ around others), as we will explain in next sections, it proves useful to develop a self-consistent and comprehensive methodology that can be used to calculate the HZ of any system with more than one stellar component. The latter constitutes the main goal of this paper. We consider the HZ to be a region where an Earth-like planet (that is, a rocky planet with a $\text{CO}_2/\text{H}_2\text{O}/\text{N}_2$ atmosphere and sufficiently large water content) can permanently maintain liquid water on its solid surface. This definition of the HZ assumes that similar to Earth, the planet has a dynamic interior and a geophysical cycle similar to Earth’s carbonate silicate cycle that naturally regulates the abundance of CO_2 and H_2O in its atmosphere. The boundaries of the HZ are then associated with an H_2O -dominated atmosphere for its outer boundary and a CO_2 -dominated atmosphere for its inner limit. Between those limits on a geologically active planet, climate stability is established by a feedback mechanism through which the concentration of CO_2 in the atmosphere varies inversely with planetary surface temperature.

It is important to note that in a multiple star system, the close approach of each star of the system to a planet can substantially affect the contribution of that star to the overall flux received by the planet. Also, the interaction between the star and the planet can affect the orbital motion of the planet, and therefore, its habitability. This all implies that the (instantaneous) shape of the HZ in a multiple star system will vary during the motion of the stars. In the next sections, we discuss this in more detail and explain how our methodology treats this matter properly.

In Section 2, we present the generalization of the calculation of a Binary HZ to a system of N stars. In Section 3, we demonstrate the time-variation of the HZ in a multiple star system by applying our methodology to some of the systems from the *Kepler* catalog. Motivated by the *Habitable Zone Gallery* (hzzgallery.org, Kane & Gelino 2012) which provides information about the HZ around single stars, we present in section 4 our fully interactive website for calculating the HZ in binary and multiple star systems. We also demonstrate in this section how to use our website by calculating the HZ of two analytical solutions of the three-body problem. In Section 5, we conclude this study by summarizing the results.

2. Calculation of the Habitable Zone

As mentioned in the previous section, we consider the habitable zone to be the region where a fictitious Earth-like planet with a $\text{CO}_2/\text{H}_2\text{O}/\text{N}_2$ atmosphere, and similar geophysical and geodynamical properties as those of Earth can maintain liquid water on its solid surface. As the capability of retaining liquid water depends on the planet’s equilibrium temperature, and because this temperature depends on the total flux received by the planet, the statement above is equivalent to considering the HZ to be the region where the total flux received at the top of the atmosphere of

a fictitious Earth-like planet is equal to that of Earth received from the Sun. To calculate this flux for a star in a multiple star system, we generalize the methodology presented by HK13 and KH13 (which has been developed for binary star systems) to systems with N number of stars. Using equation (1) in KH13 and equation (3) in HK13, that implies,

$$F_{\text{total}} = \sum_{i=1}^N W_i(T_{\text{star}}) \frac{L_i/L_{\odot}}{d_i^2}. \quad (1)$$

In this equation, F_{total} is the total flux received by the planet, L_i is the luminosity of star i in units of the solar luminosity (L_{\odot}), d_i is the distance of the planet to the i -th star in astronomical units (AU), and $W_i(T_{\text{star}})$ is the spectral weight factor which accounts for the different spectral energy distribution of the i -th star compared to the Sun. The quantity T_{star} is the effective stellar temperature.

The value of the spectral weight factor $W(T)$, in addition to the star's effective temperature, depends also on the models of the Sun's HZ. We consider the models recently developed by Kopparapu et al. (2013a,b) for which the spectral weight factor of a star with an effective temperature in the range of $2600 \text{ K} \leq T_{\text{star}} \leq 7200 \text{ K}$, is given by (HK13 and KH13)

$$W(T_{\text{star}}) = \left[1 + \alpha(T_S) d_{\text{Sun}}^2 \right]^{-1}. \quad (2)$$

In this equation, $T_S = T_{\text{star}} - 5780 \text{ K}$ is the star's temperature-difference compared to the Sun, and

$$\alpha(T_S) = aT_S + bT_S^2 + cT_S^3 + dT_S^4. \quad (3)$$

The quantities a, b, c , and d in equation (3) are constant coefficients with values that depend on the conditions that determine the inner and outer boundaries of the Sun's HZ. Table 1 shows these values.

As mentioned earlier, to calculate the HZ of a multiple star system, we compare the total flux received by a fictitious Earth-like planet with that received by Earth from the Sun. From equation (1), that means,

$$\sum_{i=1}^N W_i(T_{\text{star}}) \frac{L_i/L_{\odot}}{d_i^2} = \frac{L_{\odot}}{l_{\text{x-Sun}}^2}, \quad (4)$$

where $x = (\text{In}, \text{Out})$, and $l_{x-\text{Sun}}$ denotes the boundaries of the Sun’s HZ. To determine the location and range of the HZ of a multiple star system, the distances d_i have to be calculated for different values of $l_{x-\text{Sun}}$ by solving a set of differential equations corresponding to the motion of the stellar N -body system along with the algebraic equation (4).

To determine the values of $l_{x-\text{Sun}}$, we follow HK13 and KH13, and consider a *narrow* HZ corresponding to the region between the runaway greenhouse and the maximum greenhouse limits in the most recent Sun’s HZ mode by Kopparapu et al. (2013a,b). As this model does not include cloud feedback, the boundaries of the narrow HZ in our definition do not include the feedback from clouds as well. To mimic the effects of clouds (and have a more realistic definition for the HZ), HK13 and KH13 introduced the *empirical* (nominal) HZ as the region with an inner boundary at the Recent Venus limit and an outer boundary at the limit of Early Mars in the model by Kopparapu et al. (2013a,b). These boundaries have been derived using the fluxes received by Mars and Venus at 3.5 and 1.0 Gyr ago, respectively. At these times, the two planets did not show indications for liquid water on their surfaces (Kasting et al. 1993). We follow HK13 and KH13, and consider also the empirical HZ, as the second range for determining the values of $l_{x-\text{Sun}}$. In these definitions, the locations of the HZs are determined based on the flux received by the planet (Kasting et al. 1993; Selsis et al. 2007; Kaltenegger & Sasselov 2011; Kopparapu et al. 2013a).

It is important to note that, except for some special orbital configurations of the stars (e.g., when the stars orbit the center of mass of the system so close to one another that the system’s HZ can only exist around the entire stellar system, as in HK13), it may not be possible to determine a distinct inner or outer edge for the HZ of a multiple star system. The motions of the stars cause the HZ of the system to be dynamic and change boundaries and locations as the stars move over the time. For this reason, in order to determine the location of the HZ of the system, at any given time, we consider a large grid of points over the entire system and calculate the flux at each grid point using the equation (1). We then mark those points of the grid for which the value of the total flux satisfies the following condition, as a point of the system’s HZ:

$$\frac{L_{\odot}}{l_{\text{In-Sun}}^2} \leq \sum_{i=1}^N W_i(T_{\text{star}}) \frac{L_i/L_{\odot}}{d_i^2} \leq \frac{L_{\odot}}{l_{\text{Out-Sun}}^2}, \quad (5)$$

We repeat this process for one complete orbital period of the system by increasing the time in small increments and allowing the stars to move in their orbits. When calculating the HZ, we do not consider whether the orbit of the fictitious Earth-like planet will stay stable. As explained in the next sections, we determine the stability of the HZ by direct integration of the orbit of an Earth-mass planet at different locations in the HZ. As a result, in some systems, some or all of the HZ will be dynamically unstable (see HK13 for several examples). In the following, we present a

sample of our calculations as well as the instructions to our interactive HZ-calculator website.

3. Examples

To demonstrate the application of our methodology, we calculate the HZ of two multiple stars systems KIC 4150611 and KID 5653126 from the *Kepler* space telescope catalog. As explained below, these systems have stellar and orbital characteristics that allow for exploring effects of luminosity and distance on the range of the HZ. We calculate the narrow and empirical HZs in these systems, and show the results for one complete orbit. Following HK13 and KH13, and from the model by Kopparapu et al. (2013a,b), we consider the narrow HZ (without cloud feedback) of a Sun-like star to extend from 0.97 AU to 1.67 AU, and its empirical HZ to be from 0.75 AU to 1.77 AU. Movies of the time-variation of the HZs of our systems can be found at <http://astro.twam.info/hz-multi>.

3.1. KIC 4150611

The KIC 4150611 (HD 181469, HIP 94924) is a system of five stars consisting of a triplet with an A and two K stars, and a binary with two F stars. The A-KK and FF systems form a visual pair with a separation of 1.1". The A-KK triplet has an orbital period of 94.2 days, and the orbital period of the inner KK binary is 1.522 days. The effective temperatures of the A and K stars are 8500 K and 4500 K, respectively (A. Prša, private communication). We consider here only the A-KK system and use our methodology to calculate the location and time-evolution of its HZ (given the large separation between this system and the FF binary, the effect of the latter is negligible).

As shown by equation (5), the calculation of the HZ requires the knowledge of the luminosity, semimajor axis, and spectral weight factor of each star. To calculate the semimajor axis and luminosity of the A and K stars, we consider the A star to be $1.5M_{\odot}$ (corresponding to the lower limit of the mass of a star of spectral type A) and the mass of each K star to be $0.7M_{\odot}$. Using these values of the mass combined with the orbital periods of the KK binary and A-KK system as given above, the semimajor axis of the KK binary will be 0.029 AU and that of the A-KK system will be equal to 0.58 AU. The luminosities are calculated using the mass-luminosity relation, $L = M^{3.5}$. For the values of the stellar masses considered here, the luminosity of the A star will be equal to $4.134L_{\odot}$ and that of the K stars will be $0.287L_{\odot}$. To calculate the spectral weight factor $W(T)$ for each star, we use equation (2). It is important to note that this equation is model-dependent and has been derived based on the model of the Sun's HZ by Kopparapu et al. (2013a,b), which is valid for stellar temperatures ranging from 2600 K to 7200 K. The latter means that equation (2) may not be

applicable when calculating the spectral weight factor of the A star (8500 K). However, because the purpose of our calculations is to demonstrate our methodology and how it is used to determine the HZ of multiple star systems, we assume that the model by Kopparapu et al. (2013a,b) will maintain the functional form of its temperature dependence (i.e., equation 3) for higher values of stellar temperature, and extrapolate this model to effective stellar temperatures of 8500 K. We then calculate the spectral weight factor of each star using equation (2). Table 2 shows these values for the system’s A and K stars.

Given the short period of the KK binary (1.522 days), the stand-alone HZ of this system (i.e., assuming it is isolated and not part of a triple or larger stellar system) will be only at circumbinary distances. Following the methodology by HK13, this HZ extends from 0.6 AU to 1.5 AU from the center of mass of the binary. The top-right panel of Figure 1 shows this region. The dark green in this and subsequent figures corresponds to the narrow and the light green corresponds to the empirical HZ. Similarly, assuming that the A star is isolated and not part of a multiple star system, its single-star HZ, shown in the top-left panel of Figure 1, will extend from 1.3 AU to 3.1 AU. As the distance between the A star and the center of mass of the KK binary in the A-KK system is 20 times larger than the semimajor axis of the binary K stars, one would expect that the effect of the A star on the stand-alone HZ of the KK binary, if not negligible, to be very small. However, as shown in the bottom panel of Figure 1, when these three stars are considered to be in their current orbital configuration, and assuming that the orbits are co-planar and circular, the higher luminosity of the A star dominates and causes the entire HZ around the KK binary to disappear. In this case, the HZ of the A-KK system is primarily due to the A star although the KK binary does seem to have some small effect. A movie of the HZ of this system can be found at <http://astro.twam.info/hz-multi>.

To determine the orbital stability of an Earth-like planet in the HZ of the A-KK system, we distributed 100,000 non-interacting Earth-mass objects between 0.5 AU and 3 AU around the center of mass of the system, and integrated their orbits for 5000 periods of the A star using a fifth-order N-Body integrator (Cash & Karp 1990). The bodies were initially set to be in non-eccentric Keplerian orbits. The timesteps of the integrations were taken to be 1/100 of the period of the inner KK binary. Figure 2 shows the distribution of the Earth-like planets at the beginning (top panel, blue) and end (bottom panel, red) of the simulations. As shown here, at the end of the simulations, a lack of particles appears for distances smaller than 1.32 AU (shown by the vertical dashed line in Figure 2), implying that the orbit of an Earth-mass planet in these regions will be unstable. We, therefore, considered 1.32 AU as the stability limit, and have shown this by the dashed circles in Figure 1.

As mentioned above, the stability integrations were carried out for only 5000 orbits of the A star. To determine whether this time of integration was sufficient, we assumed that the triple star system of A-KK can be approximated by a binary star system with the A star as its primary and

a secondary with a mass equal to the sum of the masses of the two K stars ($0.7 + 0.7 = 1.4M_{\odot}$). We recall that the distance between the A star and the center of mass of the KK binary is 20 times larger than the binary semimajor axis. In this *auxiliary* binary system, an Earth-mass planet in the HZ will have a circumbinary orbit. As shown by Dvorak (1986), Dvorak et al. (1989), and Holman & Wiegert (1999), for such planetary orbits, the stability limit is given by

$$a_{\min} = a \left(1.60 + 5.10 e - 2.22 e^2 + 4.12 \mu - 4.27 e \mu - 5.09 \mu^2 + 4.61 e^2 \mu^2 \right), \quad (6)$$

where a_{\min} is the minimum semimajor axis for a planetary orbit to be stable, a is the binary semimajor axis, e is the binary eccentricity and $\mu = M_{\text{Pr}}/(M_{\text{Pr}} + M_{\text{Sec}})$ with M_{Pr} and M_{Sec} being the masses of the primary and secondary stars, respectively. Considering that in the actual A-KK system, the orbits are circular and the A star is at 0.58 AU from the KK binary ($a = 0.58$ AU), the stability limit obtained from equation (6) is at $a_{\min} = 1.39$ AU. This value is in good agreement with the 1.32 AU stability limit obtained from our numerical simulations, indicating that stability integrations have been carried out for a sufficient amount of time.

3.1.1. Effect of the eccentricity of the A star

The fact that the high luminosity of the A star stripped the KK binary from its HZ motivated us to examine how the HZ of the entire triple system would change, and at what stage the HZ around the KK binary would re-appear, had the A star been at farther distances. We, therefore, increased the radial distance of the A star from the center of mass of the system, and determined the smallest distance ($r_1 = 2.8$ AU) for which the inner edge of the empirical HZ re-appeared around the KK binary. We continued increasing the radial distance of the A star until the smallest value ($r_2 = 6.45$ AU) for which the outer boundary of the empirical HZ of the KK binary re-appeared. Beyond this distance, the two HZs of the A star and KK binary will separate. To study the HZ of the triple system in the intermediate distances, we considered two cases. In the first case, we assumed the closest and farthest distances of the A star to be $0.5r_1$ and $1.5r_1$, respectively, and calculated the semimajor axis and eccentricity of an elliptical orbit for the A star for which these distances could be the periastron and apastron ($a_1 = 2.8$ AU, $e_1 = 0.5$). Figure 3 shows four snapshots of the HZ of this system during the orbital motion of the A star. From top-right panel and in a counter-clockwise rotation, the panels correspond to the A star to be at angles 0° , 63° , 110° , and 180° with respect to the horizontal line passing through zero on the vertical axis. The dashed circles correspond to the outer boundaries of planetary stability (planets interior to the dashed circles will be stable). Around the A star, this boundary is at 0.34 AU, and around the KK binary is at 0.32 AU. The inner boundary of stability around the entire system is at approximately 10.18 AU (outside this limit, planets will have stable orbits). As shown here, while the A star is still the dominating factor in

establishing the boundaries of the narrow HZ, there are distances where the inner region of the empirical HZ of the KK binary is solely due to the luminosities of its two stars. For a movie of the HZ of this system see <http://astro.twam.info/hz-multi>.

In the second case, we considered the closest and farthest distances of the A star to be $0.5r_2$ and $1.5r_2$, respectively. The corresponding elliptical orbit of the A star in this case has a semimajor axis of 5.48 AU and an eccentricity of 0.412. Figure 4 shows the evolution of the HZ during the motion of the A star. From the top-right panel and in a counter-clockwise rotation, the panels correspond to 0° , 19° , 86° , and 180° , respectively. The outer boundaries of planetary orbit stability are at 0.8 AU around the A star and 0.77 AU around the KK binary. The inner stability limit around the entire system is at 18.95 AU. As shown here, beyond certain distances, the HZ of the KK binary reappears, and the HZ of the triple system consists of two separate HZs corresponding to those of the A star and KK binary, respectively. A movie of the HZ of this system can be found at <http://astro.twam.info/hz-multi>.

3.2. KID 5653126

The A-KK triplet in the multiple star system KIC 4150611 provided an interesting case for studying how the HZ of a binary can be affected by a highly luminous farther companion. To study the reverse situation, that is, the possible effect of a less luminous farther star on the HZ of a binary with more luminous components, we considered the hierarchical triple star system KID 5653126. This system consists of a close binary (hereafter labeled as A and B) with a period of 38.5 days and a farther companion (hereafter labeled as C) orbiting the AB binary in an 800-day orbit. The stellar properties of this system are unknown. To ensure that the farther companion would be a less luminous star, we consider the star A to be similar to the primary of the Kepler 47 system and stars B and C to be similar to the primary and secondary stars of Kepler 64, respectively. Table 3 shows the values of the mass, luminosity, and effective temperatures of these stars. From the values of the mass and orbital periods of the system, the AB binary will have a semimajor axis of $a_{AB} = 0.31$ AU and that of star C, with respect to the center of mass of the binary system, will be $a_C = 2.42$ AU. In contrary to the A-KK triplet in the KIC 4150611 system, the separation of star C is only 7.8 times larger than the semimajor axis of the inner binary AB, implying that this star may have a noticeable effect on the HZ of the binary system.

Figure 5 shows the HZ of the system when the binary AB and star C are in circular orbits. Starting from the upper-right panel and counter-clockwise, the figures show the evolution of the HZ during one revolution of the star C around the binary when this star is at 0° , 60° , 120° , 180° , 240° and 330° , respectively. As shown here, while the HZ of the system is primarily due to the AB binary, the radiation from star C excludes the region around this star from the system’s narrow HZ

and slightly extends the empirical HZ of the AB binary to farther distances (movies of the HZ at <http://astro.twam.info/hz-multi>).

To determine the stability of an Earth-like planet in the HZ of the KID 5653126 system, similar to the case of KIC 4150611, we distributed a large number of non-interacting, Earth-mass planets around the center of mass of the AB-C system, and integrated their orbits for 10000 orbital periods of the star C using the N-body integrator explained in section 3.1. Figure 6 shows the distributions of the Earth-mass planets at the beginning and end of the integrations. The top panel of this figure corresponds to the stability around the entire system and the bottom panel is for the stability around the star C. As shown here, the stability limit around the system’s center of mass is at approximately 5.225 AU (shown by a dashed line in the top panel of Figure 6 and by a dashed circle in Figure 5) indicating that the majority of the HZ of the system is unstable. As indicated by the bottom panel of Figure 6, however, a small region of stability exists interior to 0.348 AU around the star C (shown by a dashed line in the bottom panel of Figure 6 and a dashed circle around this star in Figure 5) where an Earth-mass planet can have a stable orbit in a small portion of the empirical HZ around this star.

To determine whether the above-mentioned integration time was sufficient for calculating the stability limit around the entire three stars, we approximated the AB-C system with a circular P-type binary. In this binary, the mass of the primary star is equal to the sum of the masses of stars A and B, and the binary semimajor axis is 2.42 AU. Using equation (6), the stability limit of this P-type system will be at ~ 5 AU, which is in a very good agreement with the 5.225 AU that was obtained from direct integrations.

To examine whether the time of the integration was sufficient for calculating the stability limit around the star C, we approximate the AB-C system with an S-type binary, considering star C to be the primary star. As shown by Holman & Wiegert (1999) and Rabl & Dvorak (1988), the critical stability limit around each star of an S-type binary (interior to which a planet will have a long-term stable orbit) can be calculated using

$$a_{\max} = a \left(0.464 - 0.38 \mu - 0.631 e + 0.586 \mu e + 0.15 e^2 - 0.198 \mu e^2 \right). \quad (7)$$

Considering a circular binary with a semimajor axis of 2.42 AU and a mass-ratio of $\mu = (M_A + M_B)/(M_A + M_B + M_C)$, the outer boundary of the stable region around star C will be at 0.328 AU. This is in a very good agreement with the 0.348 AU limit obtained from direct integrations confirming that the time of integrations for our stability analysis was sufficient.

3.2.1. *Effect of the eccentricity of the star C*

The fact that during its motion around the AB binary, the star C removes part of the HZ of the system that is in its vicinity motivated us to examine how the HZ would change if the orbit of this star were eccentric. Similar to the case of KIC 4150611, we considered two cases. In the first case, we determined the values of the semimajor axis and eccentricity of star C for which this star would break away from the inner part of the empirical HZ of the system while having a periastron distance equal to 2.42 AU and an apastron interior to the outer edge of the system’s empirical HZ. In this case $a_C = 3.01$ AU, and $e_C = 0.195$. Figure 7 shows the HZ of the system in one orbit of the star C around the binary. From the upper-right panel and in a counter-clockwise rotation, the panels correspond to star C at 0° , 60° , 180° and 309° . As shown here, the inner part of the empirical HZ of the system expands temporarily as the star C moves away from this region. The outer edge of the HZ is also extended to larger distances as this star approaches its apastron position. Figure 8 shows the outer boundary of orbital stability for Earth-mass planets around star C. Integrations were carried out for 1000 orbital periods of planet C. As indicated by the vertical dashed line, planets with semimajor axes smaller than 0.362 AU will have stable orbits around this star. Figure 7 shows this region with a dashed circle around star C. As shown in this figure, the empirical HZ around this star maintains stability for planetary orbits as this star rotates around the AB binary. For a movie of the HZ of this system, we refer the reader to the website <http://astro.twam.info/hz-multi>.

In the second case, we considered the star C to have a semimajor axis equal to 2.42 AU and changed the value of its orbital eccentricity until this star left the HZ of the binary ($e_C = 0.7$). Figure 9 shows this for half of the orbital period of star C. From top-right and in a counter-clockwise rotation, the panels show this star at 0° , 26° , 28° , 41° , 52° , 73° , 117° , 150° and 154° . As shown here, the motion of star C disturbs the HZ of the AB binary by either excluding regions of it that are around this star, or extending its inner and outer boundaries. The capability of the HZ of the AB binary to accommodate stable planetary orbits is also affected by the motion of the star C. Except for when this star is either entirely inside the inner boundary of the system’s empirical HZ or is outside the HZ of the AB binary, the stability of the system’s HZ is limited to only a small region around star C. When star C is separated from the AB binary, planetary stability is maintained in both HZs. However, as this star enters the inner boundary of the empirical HZ of the system, the stability region around it becomes unstable due to the perturbation of the AB binary. This all means that during the motion of the stars around their center of mass, an Earth-like planet may not maintain a long-term stable orbit in the HZ of the system. For more details, we refer the reader to the website <http://astro.twam.info/hz-multi> where movies of the time-variations of the HZs shown in figures 7 and 9 can be found.

4. Interactive Website

To streamline the calculations of the HZ in binary and multiple star systems, we have developed an interactive website where by inputting the orbital and physical properties of the stars, the HZ of the system is calculated for the time at which the stars are in the configuration that corresponds to their prescribed orbital parameters. The website can be found at

<http://astro.twam.info/hz>

Figure 10 shows a screenshot of the website. As shown on the top of the figure, the website gives the option for the calculations to be performed for a binary or a multiple star system. We chose to separate these two cases because in calculating the HZ of binary star systems, the website has the capability of using equations (6) and (7) to determine the boundaries of planetary stability, as well. However, for a stellar system with more than 2 stars, the stability limits can be obtained only by direct integration of the equation of motion of planetary bodies at different locations in the system. Also, for binary stars, the website offers the choice of setting the value of the mean-anomaly, which can be used to obtain snapshots of the HZ during the rotation of the two stars around their common center of mass.

The next set of input parameters are the effective temperature, luminosity, and mass of each star as well as the star’s position. The temperature and luminosity of a star are used to calculate its spectral weight factor and the boundary of the system’s HZ. The mass of each star is used to calculate boundaries of planetary stability in binary star systems, and for the calculation of the center of mass in multiple star systems. Since the value of the spectral weight factor and the locations of the boundaries of the HZ are model-dependent, the website offers the option to choose between three models of the Sun’s HZ: The model by Kasting et al. (1993)³, Selsis et al. (2007), and Kopparapu et al. (2013b). The remaining input parameters are for determining the range of plotting the HZ and its resolution.

After entering all parameters and choosing the options, the HZ of the system can be displayed by clicking on the "Render" button. The website has been programmed to stop the calculations and ask for reducing the resolution if the calculations take longer than 10 seconds. Once the HZ of the system is calculated, the displayed image can be saved as a vectorized PDF file, or a rasterized PNG image. Figure 10 shows as an example the input parameters and the calculated HZ of a GKM triple star system. In the next section, we show the application of the website by calculating the HZ of some interesting analytical solutions to the three-body problem. We would like to emphasize

³The calculations of the spectral weight factor for this model is carried out using the formulas given by Underwood et al. (2003).

that the systems studied in the next section have been chosen for the mere purpose of demonstrating the use of our interactive website. We, therefore, will not be concerned about the possibility of the formation of terrestrial-class planets in these systems, and the orbital stability of Earth-like bodies in their HZs (although when possible, we will address the latter).

4.1. Interesting Examples: Equilateral Three-Star System

Among the currently known solutions of the general three-body problem, only a few are stable. The most well-known stable solutions are the equilateral configurations where three stars (with different masses) rotate around their common center of mass in an equilateral triangle at all times. The orbits of the stars can be circular or elliptical. In the latter configuration, the distances between the stars vary with time whereas in the circular case, the distances stay constant.

We calculated the HZ of the system using our interactive website for different values of the mass, luminosity and temperature of the three stars, and for the model of the Sun’s HZ by Kopparapu et al. (2013a,b). Table 4 shows a sample of our systems for a circular (Figure 11) and an elliptical (Figure 12) configuration. The initial positions (X, Y) and velocities (V_X, V_Y) of the stars are also shown. Figure 11 shows four snapshots of the HZ of the circular case along with the orbits of the stars (black, solid circles) for one complete revolution of the system (from top-right panel and in a counter-clockwise rotation). Since in this configuration, the distances between the stars do not change, one would expect that for the types of the stars considered here, the mutual stellar interactions will be so small that planetary orbits maintain stability in the stars’ individual HZs. Figure 12, shows similar stars in an elliptical configurations. As shown here, although at times during their orbital motions, the stars are so far away from one another that they maintain their individual HZs, their subsequent close approaches causes the HZ of the system to change and the interactions among them may become so strong that the orbits of Earth-mass objects in the HZ will become unstable. Movies of the time-evolution of the HZ of the system can be found at <http://astro.twam.info/hz-multi>.

4.2. Interesting Examples: Three Stars in a Figure-Eight Orbit

Another interesting solution to the general three-body problem is when three equal-mass bodies revolve around their center of mass in a figure-eight orbit (Moore 1993; Chenciner & Montgomery 2000). Although such orbital configuration is unlikely to appear in nature, it would be interesting to calculate its HZ and determine how it evolves as the stars move in their orbits.

Using our interactive website, we calculated the HZ of such systems for different values of

the mass and temperature of each star. Results of stability analysis indicated that in general in a triple star system in a figure-eight orbit, the orbit of an Earth-mass planet will be stable at large distances around the entire system and in a small region around each star where the perturbations of other stars do not affect its motion. Figure 13 shows the results of these integrations for a system with three Sun-like stars ($T = 5780$ K). Integrations were carried out for 10000 orbital period of one star around the center of mass of the system. The values of the initial positions (X, Y) and velocities (V_X, V_Y) of these stars are given in Table 5. As indicated by the vertical dashed line in the figure, the regions of planetary stability are at distances larger than 3.5 (AU) around the entire system, and smaller than 0.160 (AU), around each star. Figure 14 shows the HZ of this system for one orbital period (starting from upper-right panel and counter-clockwise). The dashed circles in this figure correspond to the above-mentioned stability limits. Given the luminosities of the stars, the HZ of the system encompasses the entire triple stars system and its outer boundary is inside the stability limit. The latter implies that an Earth-like planet will not be able to maintain a stable orbit in this HZ.

Although the HZ of the three-star system in Figure 14 is dynamically unstable, the fact that small regions of stability exist in close distances around each star motivated us to calculate the HZ of the system for cool and low-mass stars. Figure 15 shows the results for three 0.25 solar-masses M dwarfs with luminosities of $0.0095 L_{\odot}$ and temperatures of $T = 2800$ K. From top-right panel and counter-clockwise, the figure corresponds to one complete revolution of the system. The integrations of the motion of Earth-mass objects indicated that the planetary stability is limited to distances larger than 2.20 AU around the entire system, and smaller than 0.101 AU around each star (the dashed circles in Figure 15). As shown here, while during the motion of the stars, the HZ of the system extends to larger distances, only a small region of the empirical HZ around each star maintains planetary stability. Movies of the time-evolution of the HZ of the system can be found at <http://astro.twam.info/hz-multi>.

5. Summary

We presented a general methodology for calculating the HZ of multiple star systems. We used the concept of spectral weight factor as introduced by HK13 and KH13, and calculated the total flux received at the top of the atmosphere of an Earth-like planet. By comparing this flux with that received at the top of Earth’s atmosphere from the Sun, we determined regions corresponding to narrow and empirical HZ in and around multiple stars systems. To demonstrate the applicability of our methodology, we calculated the HZ of two triple star systems and studied the effects of high and low luminosity stars on the HZ around the other stellar components. To streamline the calculations of HZ in binary and multiple star systems, we developed an interactive website where

by inputting the physical and dynamical properties of the stars, the HZ of the system is obtained.

We would like to note that the HZ, as calculated in this study is in fact an instantaneous HZ. In our calculations, we did not consider the effect of the eccentricity of the stellar and planetary orbits. When the orbit of the planet and/or those of the stars are eccentric, the close approaches of the stars to the planet will affect the total flux received at the top of the planet's atmosphere, and therefore changes the locations where the planet can be habitable (i.e., the boundaries of the system's HZ). In an actual system with an Earth-like planet, these effects have to be taken into consideration, and the region of the habitability of the planet has to be determined by averaging the flux received by the planet over the longest orbital period of the system. Such calculations have to be applied to actual systems in a case by case basis.

We would like to thank the anonymous referee for his/her constructive comments which have improved our manuscript. Tobias Müller received financial support from the Carl-Zeiss-Stiftung. N.H. acknowledges support from the NASA ADAP grant NNX13AF20G, NASA Astrobiology Institute under Cooperative Agreement NNA09DA77 at the Institute for Astronomy, University of Hawaii, HST grant HST-GO-12548.06-A, and Alexander von Humboldt Foundation. Support for program HST-GO-12548.06-A was provided by NASA through a grant from the Space Telescope Science Institute, which is operated by the Association of Universities for Research in Astronomy, Incorporated, under NASA contract NAS5-26555. N.H. is also thankful to the Computational Physics group at the Institute for Astronomy and Astrophysics, University of Tübingen for their kind hospitality during the course of this project.

REFERENCES

- Anglada-Escudé, G., Arriagada, P., Vogt, S. S., et al. 2012, *ApJ*, 751, L16
- Batten, A. H., Fletcher, J. M. & MacCarthy, D. G. 1989, in *STAR CATALOGS, SPECTROSCOPIC BINARY STARS, ORBITAL ELEMENTS*, Publications of the Dominion Astrophysical Observatory Victoria, 17, 1
- Cash, J. R. & Karp, A. H. 1990, *ACM Transactions on Mathematical Software*, 16, 201
- Chenciner, A. & Montgomery, R. 2000, *Ann. Math.*, 152, 881
- Cochran, W. D., Hatzes, A. P., Butler, R. P. & Marcy, G. W., 1997, *ApJ*, 483, 457
- Delfosse, X., Bonfils, X., Forveille, T., et al. 2013, *A&A*, 553, A8
- Duquennoy, A. & Mayor, M. 1991, *A&A*, 248, 485

- Dvorak, R. 1986, A&A, 167, 379
- Dvorak, R., Froeschle, C. & Froeschle, C. 1989, A&A, 226, 335
- Eggl, S., Pilat-Lohinger, E., Georgakarakos, N., Gyergyovits, M. & Funk, B., 2012, ApJ, 752, article id. 74
- Eggl, S., Pilat-Lohinger, E., Funk, B., Georgakarakos, N. & Haghhighipour, N. 2013, MNRAS, 428, 3104
- Haghhighipour, N. & Kaltenegger, L. 2013, ApJ, 777, article id. 166
- Holman, M. J. & Wiegert, P. A. 1999, AJ, 117, 621
- Kaltenegger, L., & Sasselov, D. 2011, ApJ, 736, L25
- Kaltenegger, L. & Haghhighipour, N. 2013, ApJ, 777, article id. 165
- Kane, S. R. & Hinkel, N. R., 2013, ApJ, 762, article id. 7
- Kane, S. R. & Gelino, D., 2012, PASP, 124, 323
- Kasting, J. F., Whitmire, D. P. & Reynolds, R. T. 1993, Icarus, 101, 108
- Kopparapu, R. K., Ramirez, R., Kasting, J. F., Eymet, V., Robinson, T. D., Mahadevan, S., Terrien, R. C., Domagal-Goldman, S., Meadows, V. & Deshpande, R. 2013a, ApJ, 765, article id. 131
- Kopparapu, R. K., Ramirez, R., Kasting, J. F., Eymet, V., Robinson, T. D., Mahadevan, S., Terrien, R. C., Domagal-Goldman, S., Meadows, V. & Deshpande, R. 2013b, ApJ, 770, article id. 82
- Liu, H-G., Zhang, H. & Zhou, J-L., 2013, ApJ, 767, L38
- Mason, P. A., Zuluaga, J. I., Clark, J. M. & Cuartas-restrepo, P. A. 2013, ApJ, 774, article id. L26
- Morre, C. 1993, Phys. Rev. Lett., 70, 3675
- Quarles, B., Musielak, Z. E. & Cuntz, M., 2012, ApJ, 750, article id. 14
- Rabl, G. & Dvorak, R. 1988, A&A, 191, 385
- Rein, H. 2012, (arXiv 1211.7121)
- Schwamb, M. E., Orosz, J. A., Carter, J. A., et al. 2013, ApJ, 768, article id. 127

Selsis, F., Kasting, J. F., Levrard, B., Paillet, J., Ribas, I. & Delfosse, X. 2007, *A&A*, 476, 1373

Slawson, R. W., Prša, A., Welsh, W. F., et al. 2011, *AJ*, 142, article id. 160

Underwood, D. R., Jones, B. W., Sleep, P. N. 2003, *IJAsB*, 2, 289

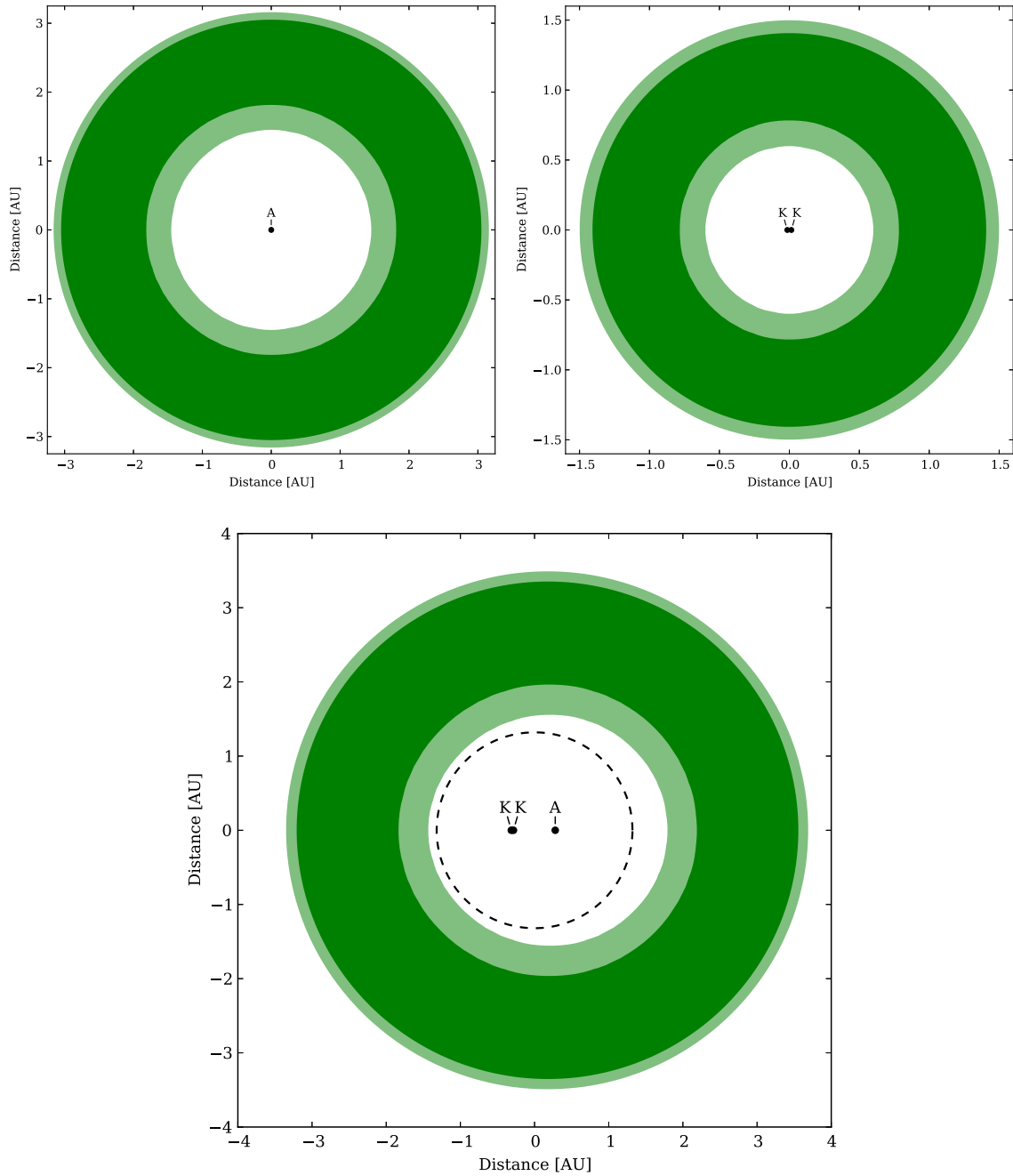


Fig. 1.— Graphs of the HZs of the A-KK triplet in the KIC 4150611 system and its components. The top-left panel shows the HZ of the A star, the top-right panel shows that of the KK binary, and the bottom panel shows the HZ of the A-KK triple star system. Here and in subsequent figures, the dark green corresponds to the narrow and the light green corresponds to the empirical HZs. The dashed circle shows the boundary of stability. Interior to this boundary, planetary orbits will become unstable. A movie of the HZ of this system can be found at <http://astro.twam.info/hz-multi>.

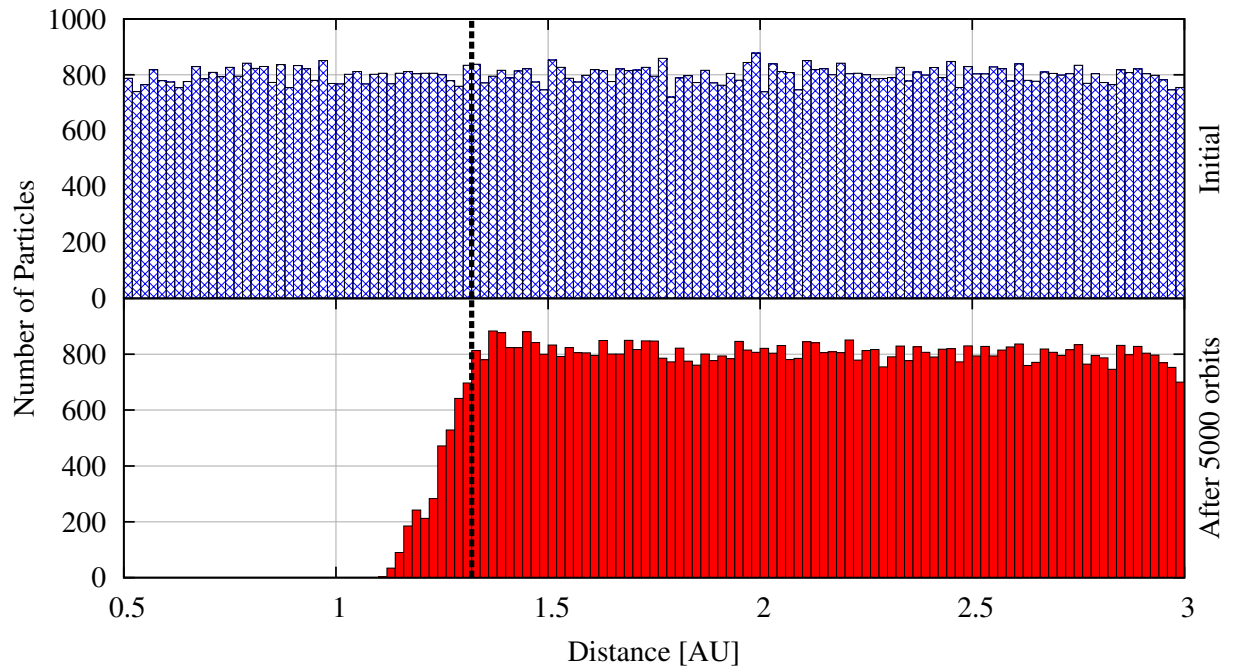


Fig. 2.— Results of the integrations of the orbits of non-interacting Earth-mass planets around the center of mass of the KIC 4150611 system. The top panel (blue histogram) shows the initial distribution of planets and the bottom panel (red histogram) corresponds to their distribution after integrating their orbits for 5000 orbital periods of star A around the KK binary. The dashed line shows the boundary of orbital stability at 1.32 AU.

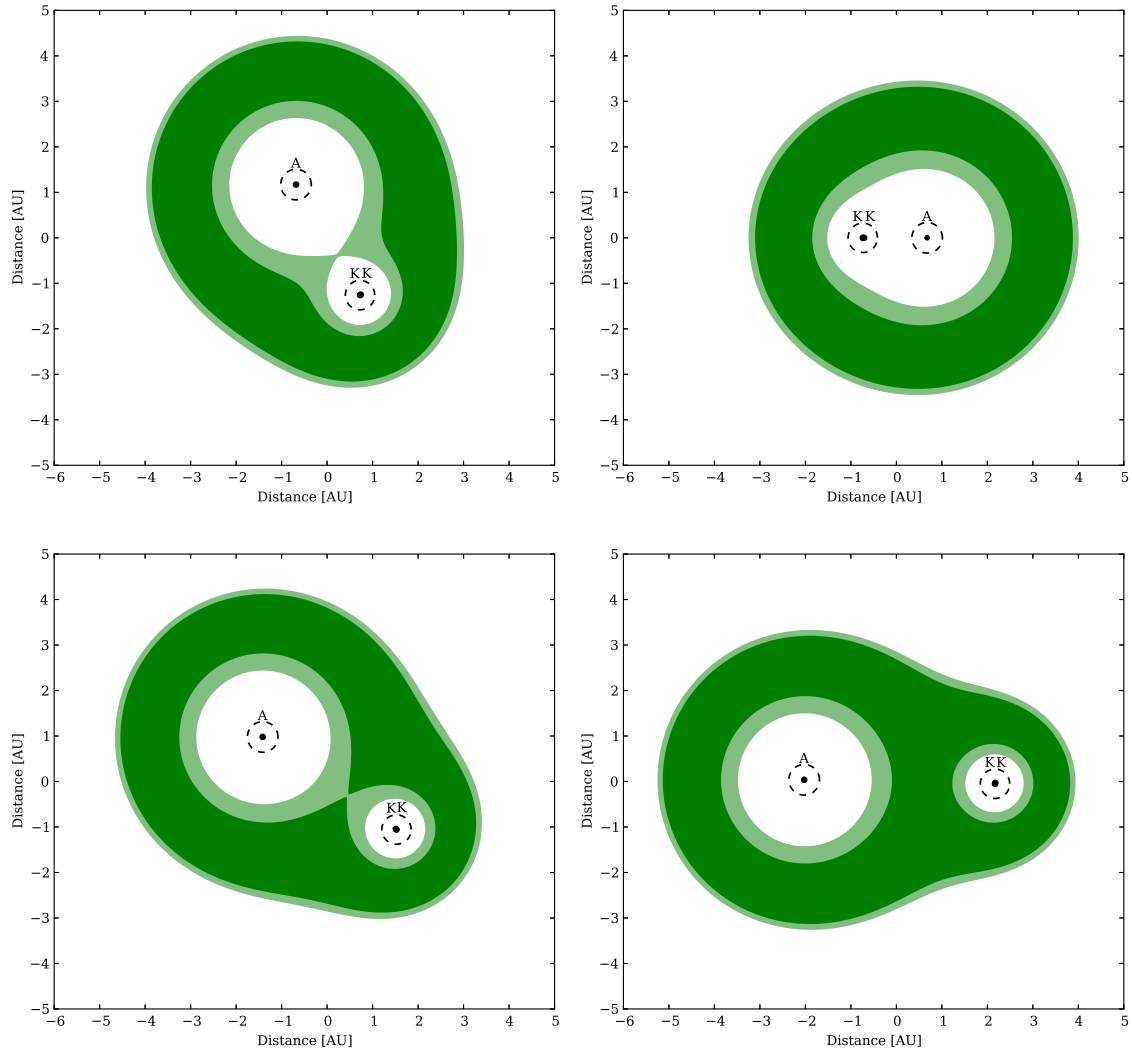


Fig. 3.— The time-evolution of the HZ of the A-KK triplet in the KIC 4150611 system when the orbit of the A star has a semimajor axis of 2.8 AU and an eccentricity of 0.5. From top-right panel and in a counter-clockwise rotation, the panels correspond to the A star being at 0° , 63° , 110° , and 180° with respect to the horizontal line passing through zero on the vertical axis. The dashed circles correspond to the outer boundary of the stability of planetary orbits. A movie of the HZ of this system can be found at <http://astro.twam.info/hz-multi>.

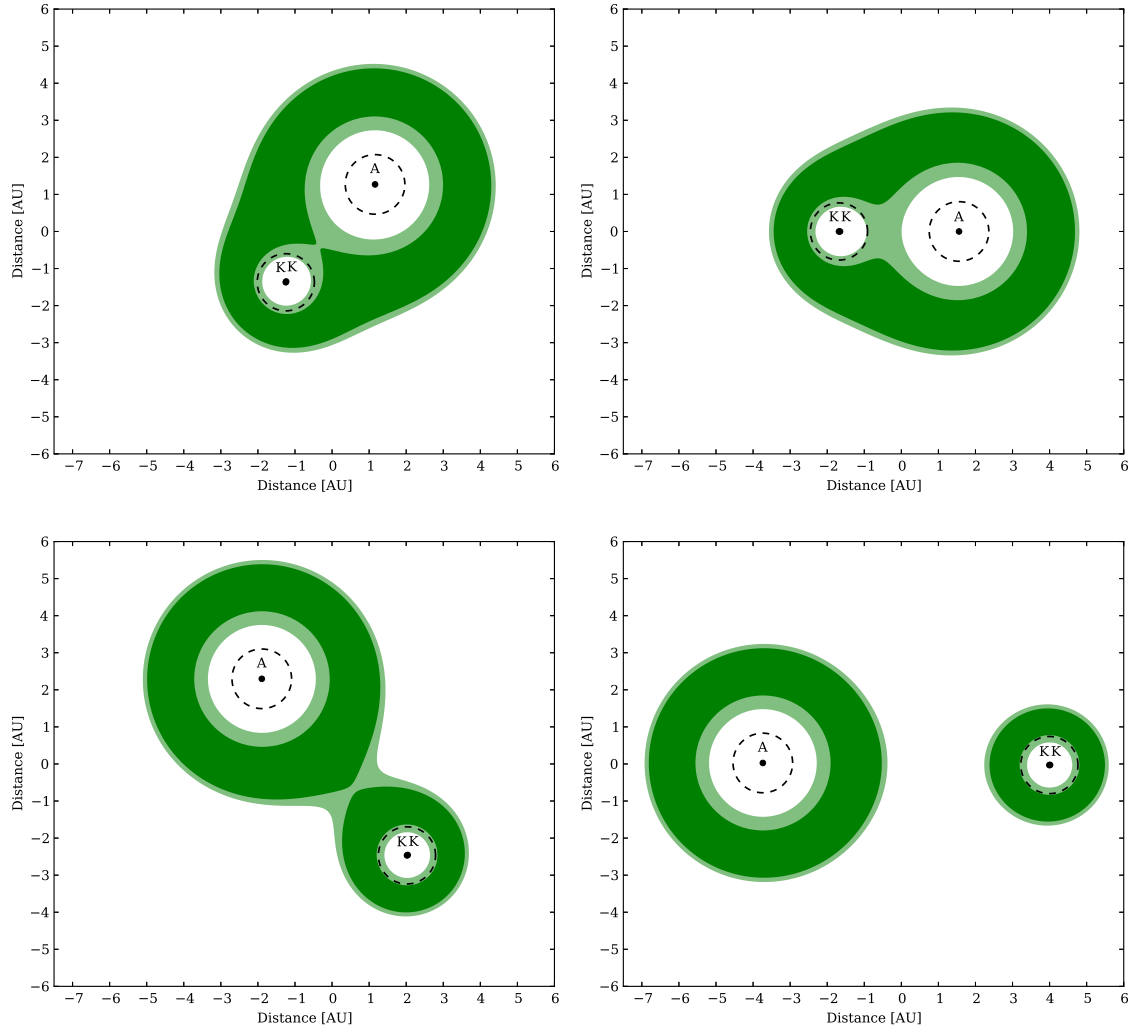


Fig. 4.— The time-evolution of the HZ of the A-KK triplet in the KIC 4150611 system when the orbit of the A star has a semimajor axis of 5.48 AU and an eccentricity of 0.412. From top-right panel in a counter-clockwise rotation, the panels correspond to the A star being at 0° , 19° , 86° , and 180° with respect to the horizontal line passing through zero on the vertical axis. The dashed circles correspond to the outer boundary of the stability of planetary orbits. A movie of the HZ of this system can be found at <http://astro.twam.info/hz-multi>.

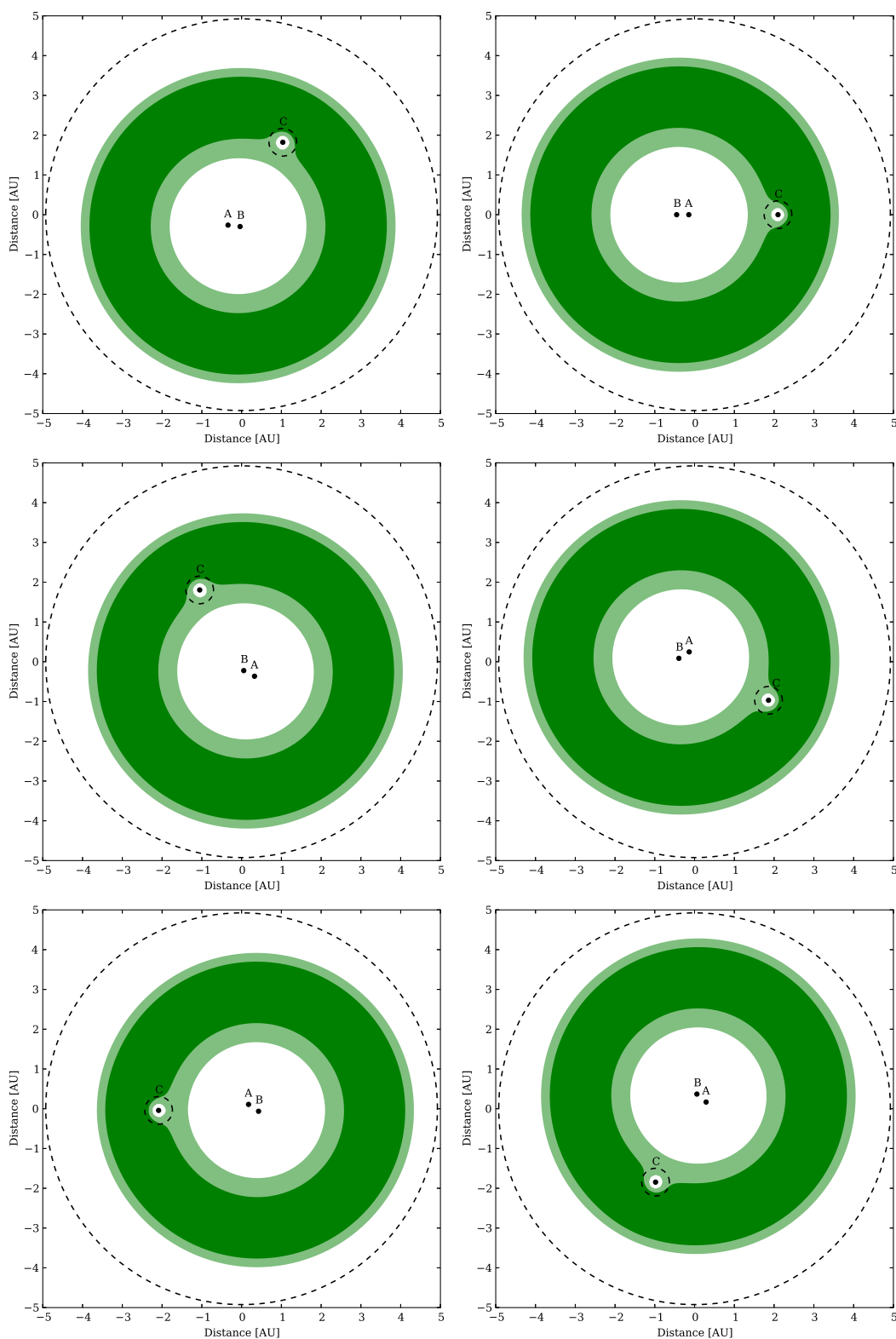


Fig. 5.— Graphs of the HZ of the KID 5653126 system when the three stars are in circular orbits. From top-right panel and counter-clockwise, the figures show the changes in the boundaries of the HZ during one revolution of the star C when this star is at 0° , 60° , 120° , 180° , 240° and 330° , respectively. The dashed circles corresponds to the limits of planetary orbit stability (see figure 6). A movie of the HZ of this system can be found at <http://astro.twam.info/hz-multi>.

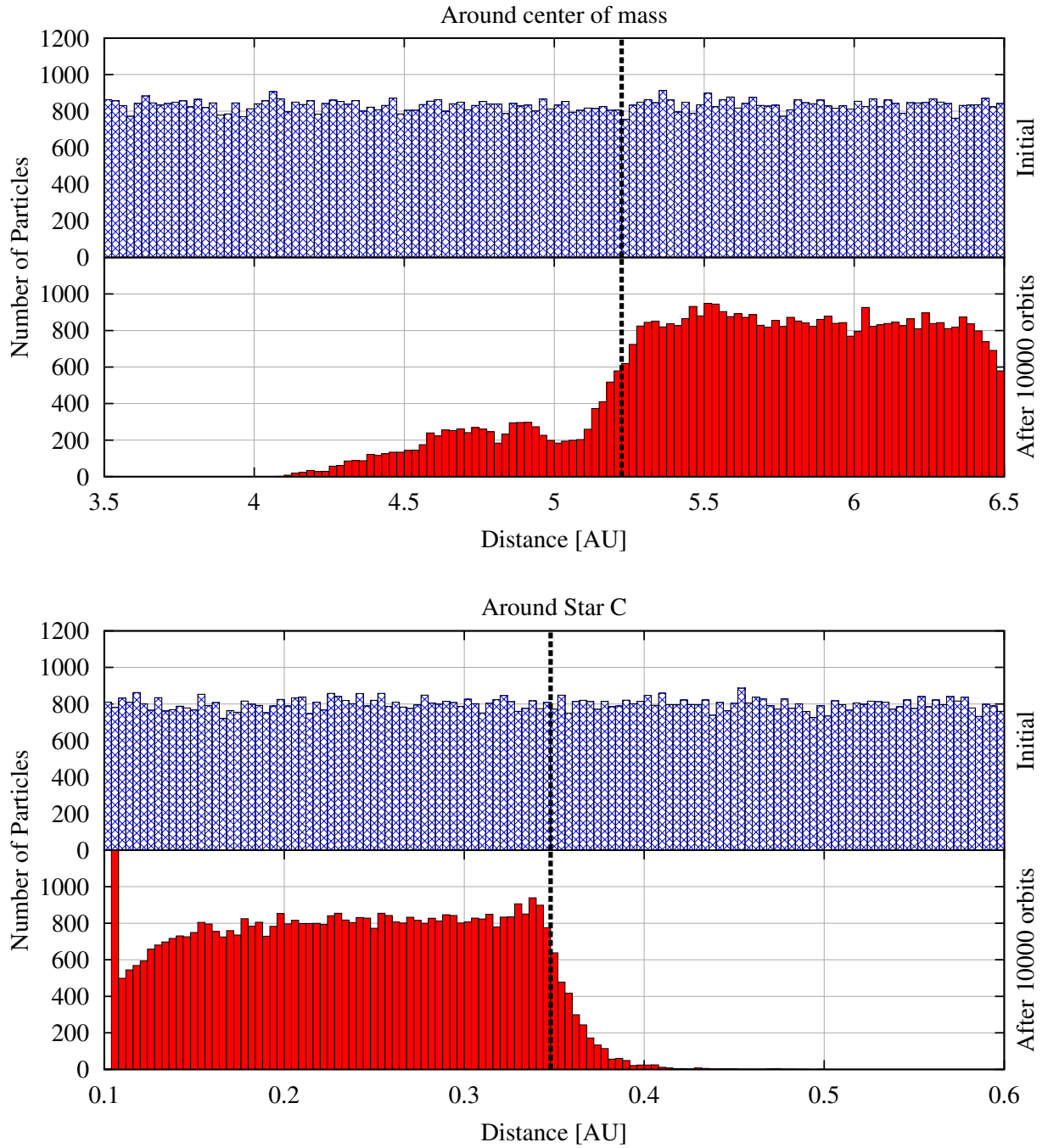


Fig. 6.— Results of the integrations of non-interacting Earth-mass planets around the center of mass of the KID 5653126 system (top) and around the star C (bottom). In each panel, the upper graph (blue histogram) shows the initial distribution of the planets and the lower graph (red histogram) corresponds to their distribution after integrating their orbits for 10000 orbital periods of the star C around the binary AB. The dashed line shows the boundary of orbital stability at 5.225 AU around the center of mass, and at 0.348 AU around star C.

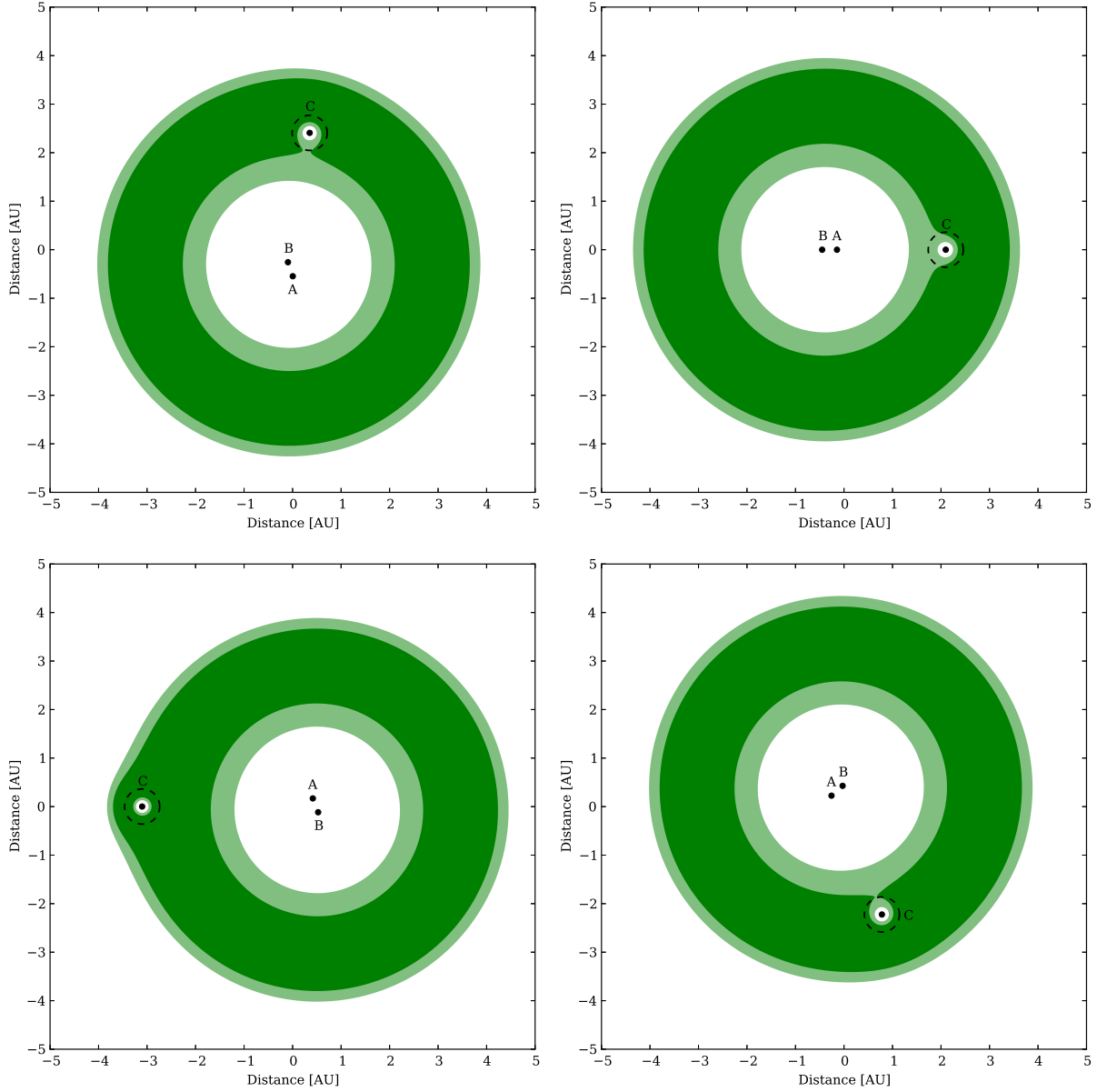


Fig. 7.— Graphs of the HZ of the KID 5653126 system when the star C has a semimajor axis of 3.01 AU and an eccentricity of 0.195. From top-right panel and in a counter-clockwise rotation, the panels correspond to the star C being at 0° , 60° , 180° and 309° , respectively. A movie of the HZ of this system can be found at <http://astro.twam.info/hz-multi>.

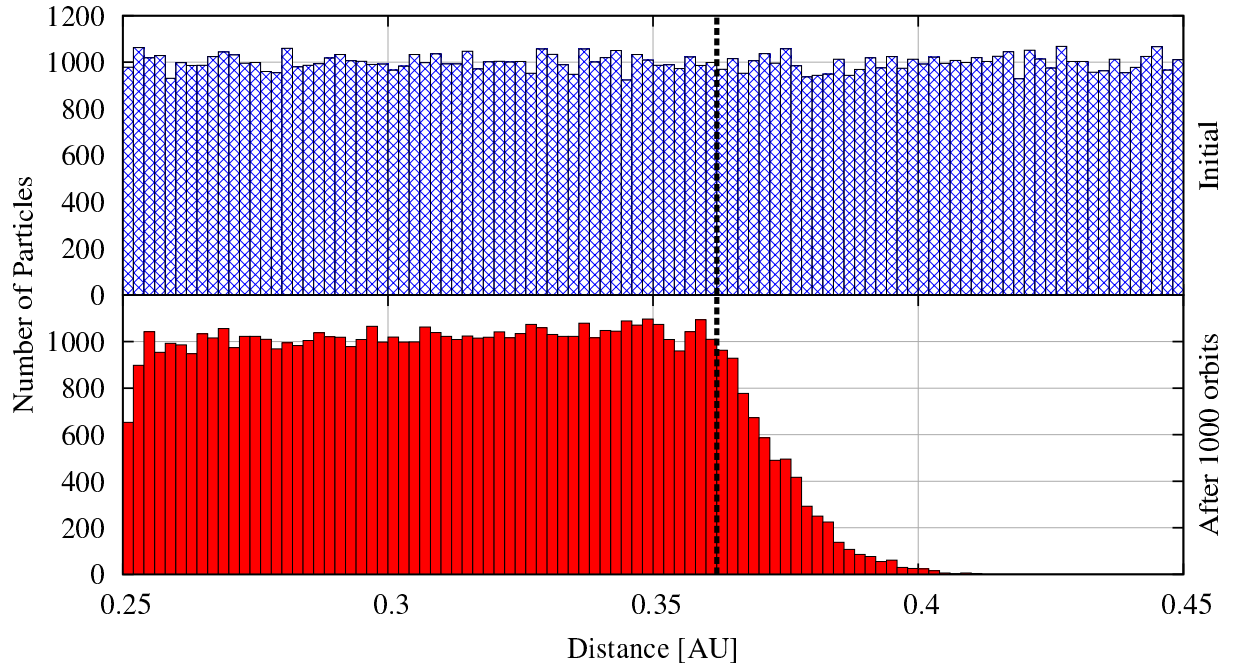


Fig. 8.— Results of the integrations of non-interacting Earth-mass planets around star C in the system of Figure 7. The upper panel (blue histogram) shows the initial distribution of the planets and the lower panel (red histogram) corresponds to their distribution after integrating their orbits for 10000 orbital periods of star C. The dashed line shows the outer boundary of orbital stability at 0.362 AU.

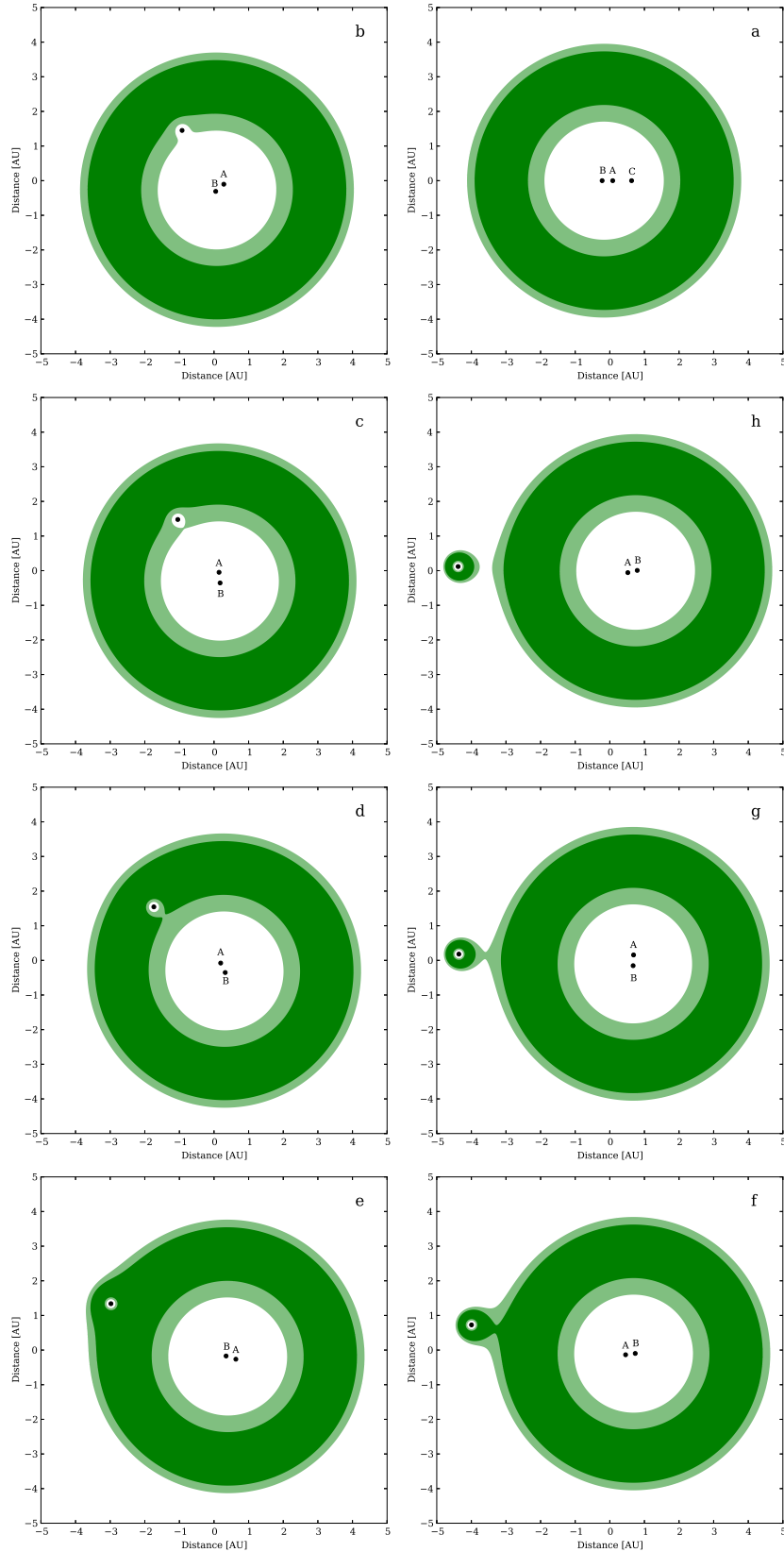


Fig. 9.— Graphs of the HZ of the KID 5653126 system when the star C has a semimajor axis of 2.42 AU and an eccentricity of 0.7. From top-right panel and in a counter-clockwise rotation (from a to h), the panels correspond to the star C being at 0° , 26° , 28° , 41° , 52° , 73° , 117° , 150° and 154° , respectively. A movie of the HZ of this system can be found at <http://astro.twam.info/hz-multi>.

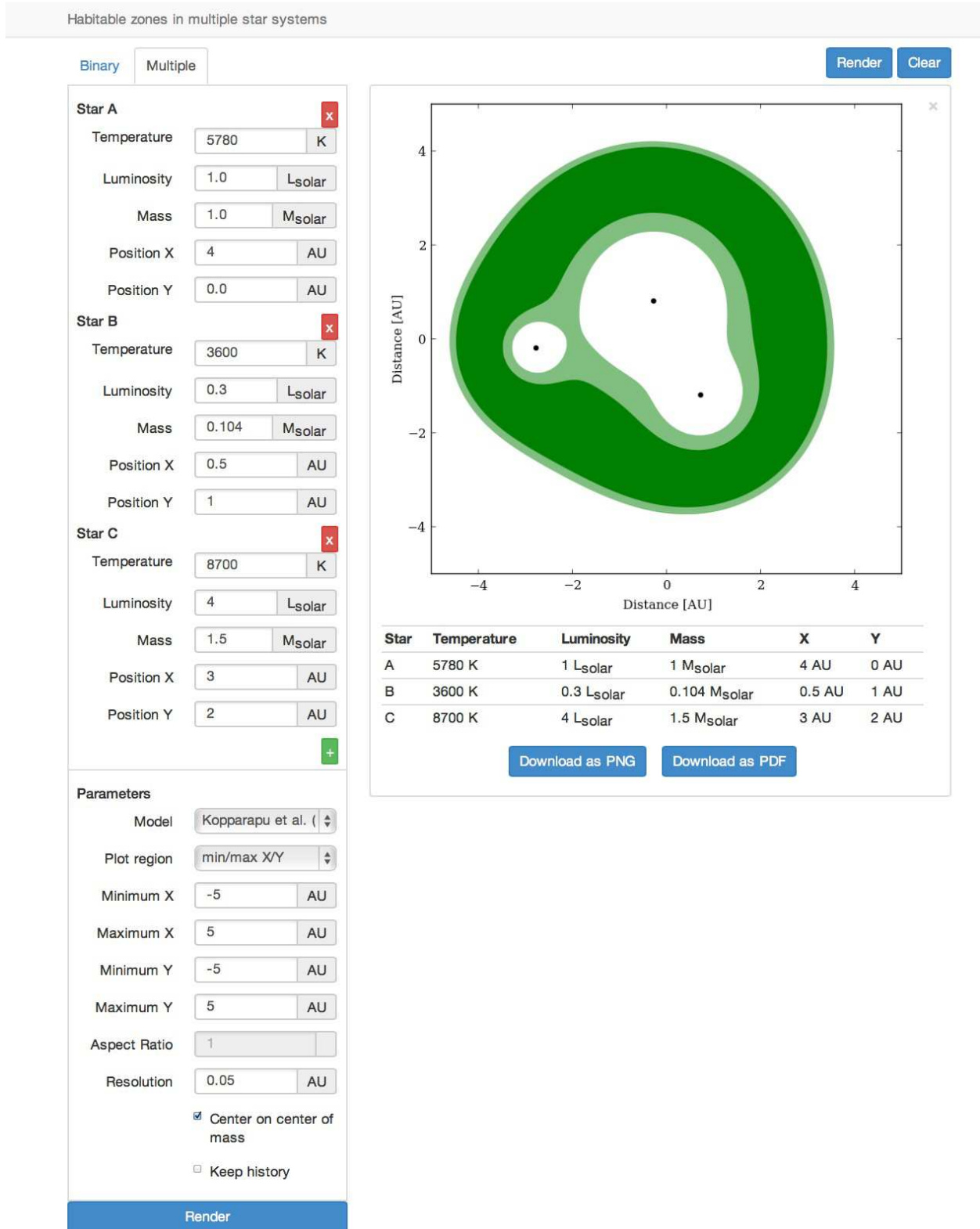


Fig. 10.— A screenshot of the interactive website <http://astro.twam.info/hz> for calculating the HZ of binary and multiple star systems.

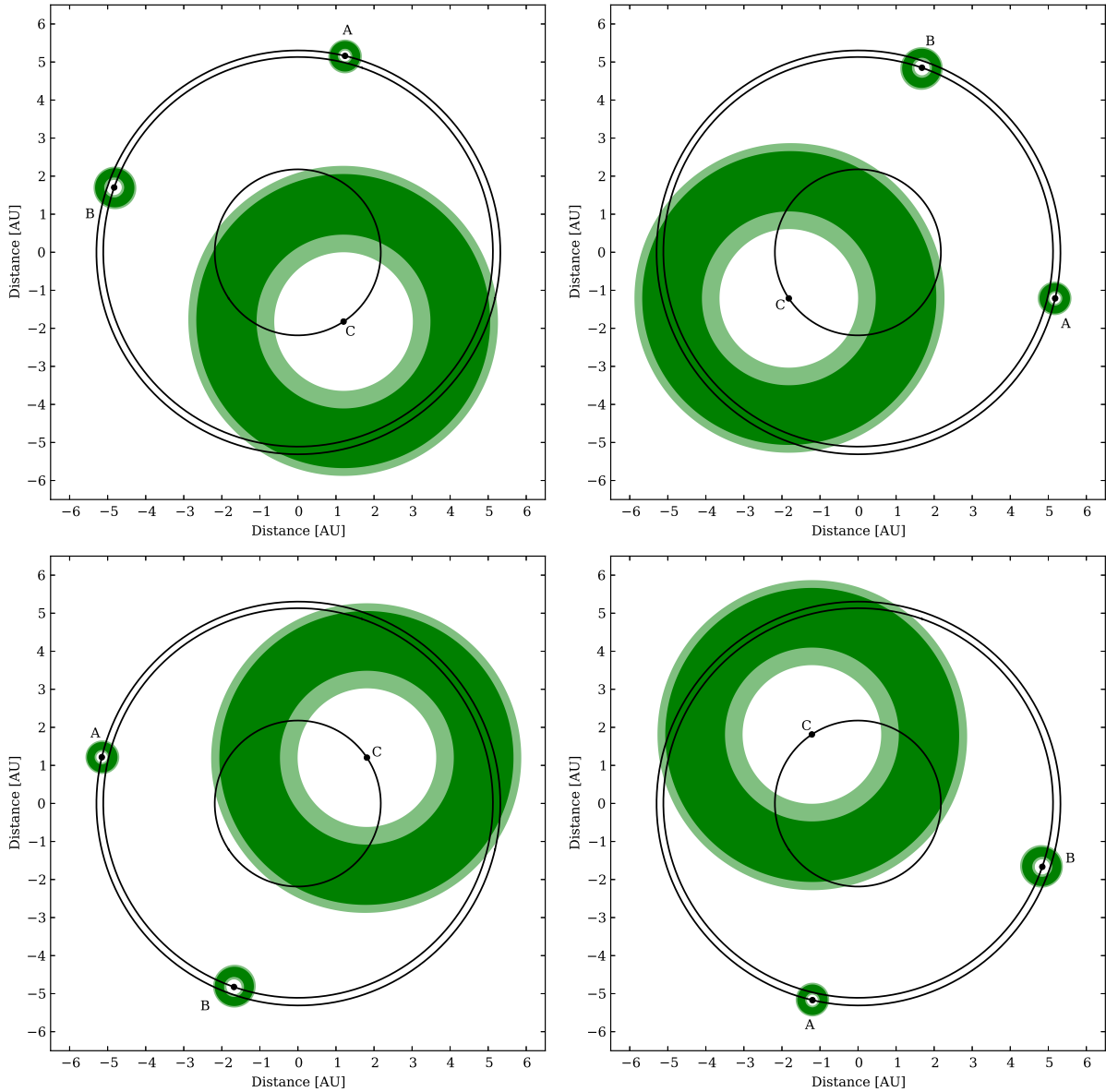


Fig. 11.— Habitable zone of a triple star system with the stars on an equilateral triangle as an analytical solution to the general three-body problem. From top-right panel and counter-clockwise, the figures show the evolution of the HZ of the system for one complete revolution around its center of mass. The stars masses, luminosities, and temperatures as well as their initial positions and velocities are given in Table 4. The orbits of the stars around the center of mass (0, 0) are shown in black. A movie of the HZ of this system can be found at <http://astro.twam.info/hz-multi>.

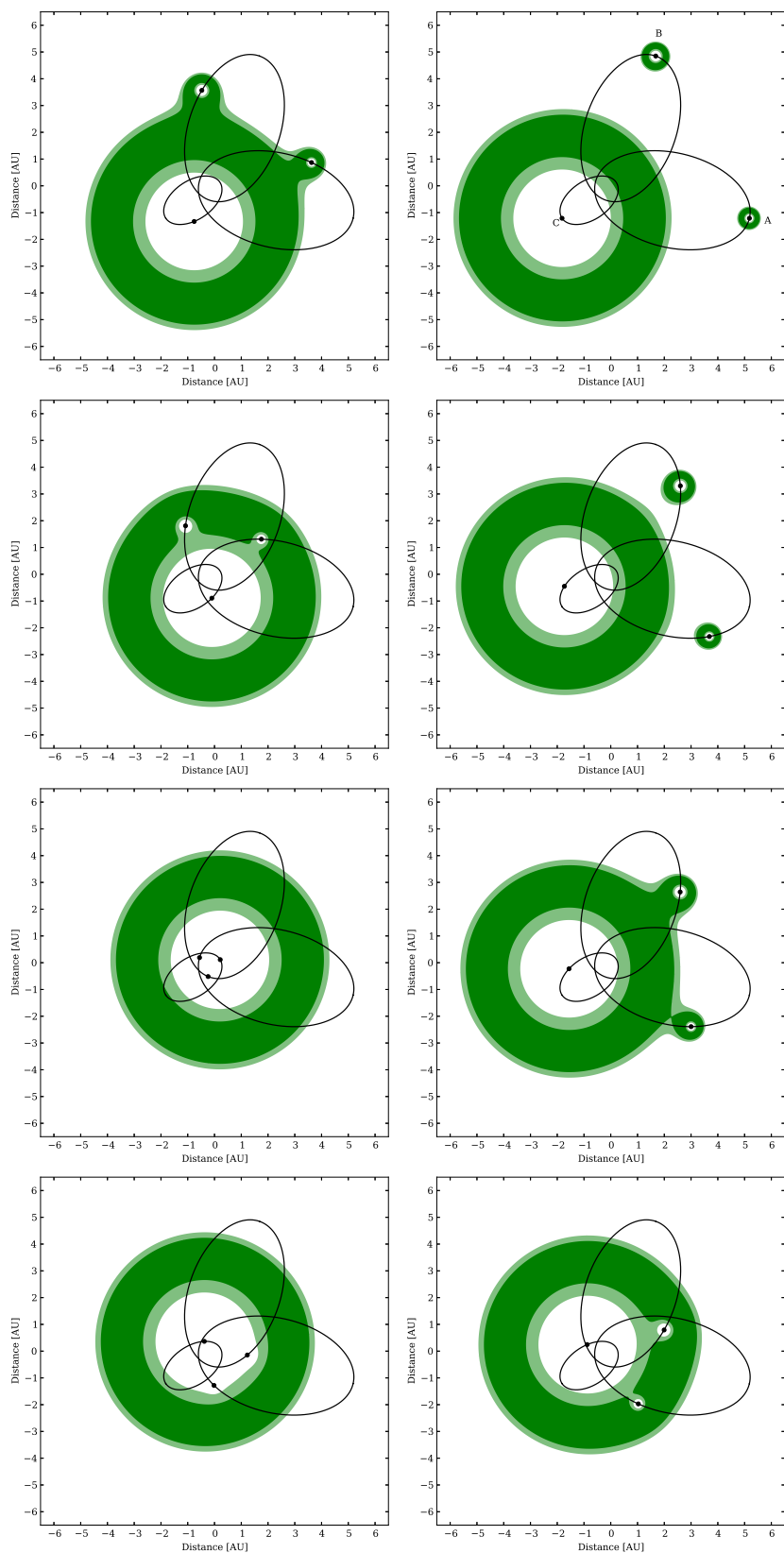


Fig. 12.— HZ of the same triple star systems as in Figure 11 with stars being in elliptical orbits. From top-right panel and counter-clockwise, the figures show the evolution of the HZ of the system for one complete revolution around its center of mass. The stars masses, luminosities, and temperatures as well as their initial positions and velocities are given in Table 4. The orbits of the stars around the center of mass (0, 0) are shown in black. A movie of the HZ of this system can be

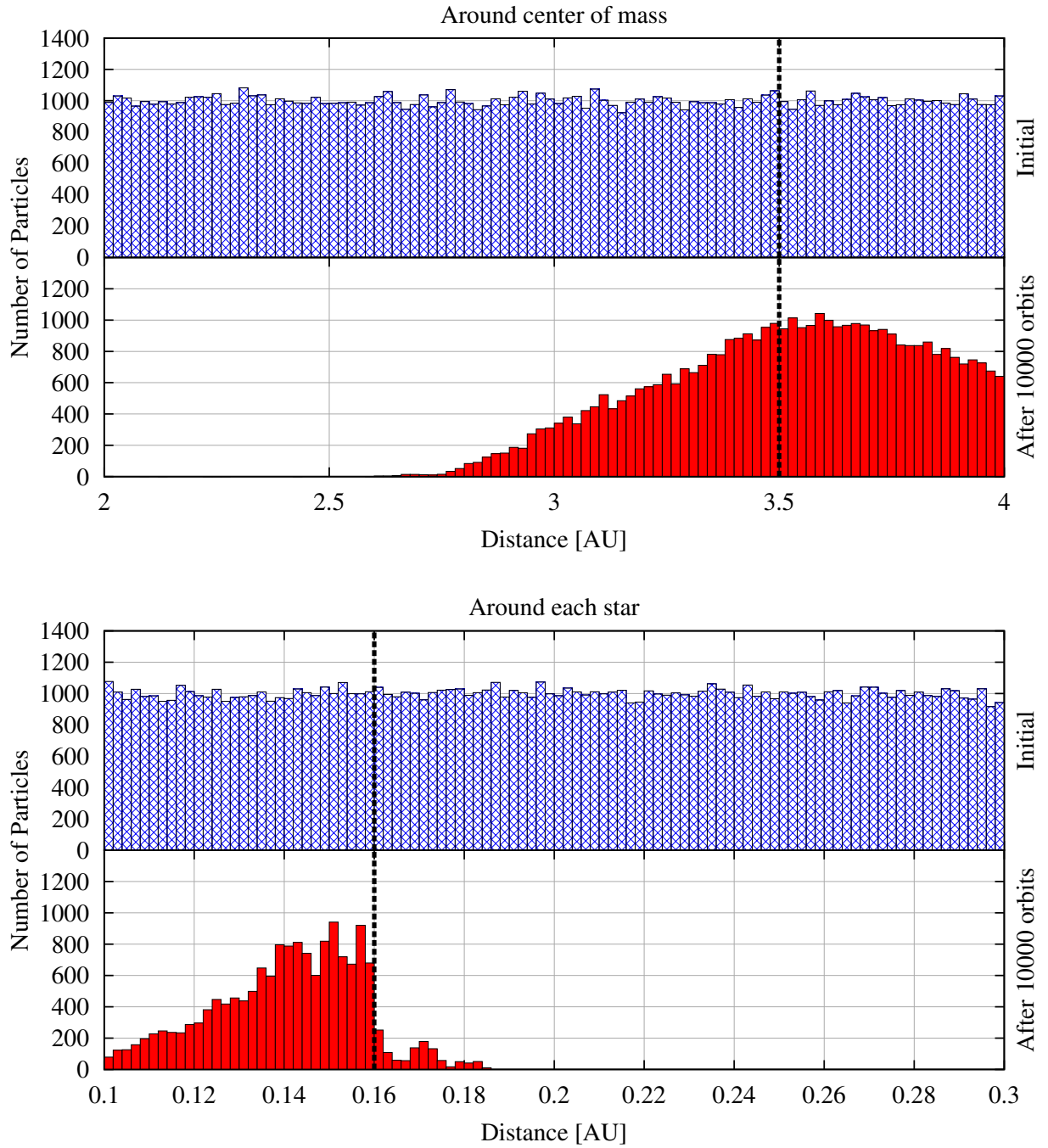


Fig. 13.— Results of the integrations of non-interacting Earth-mass planets around the center of mass of a triple stars system with Sun-like stars in a figure-eight orbit. The blue histograms show the initial distribution of the planets and the red histograms correspond to their distribution after integrating their orbits for 10000 orbital periods of one star around the center of mass of the system (the orbital periods of all stars around the center of mass are identical). As shown here, Earth-mass planets initially at distances larger than 3.5 AU (top panel) and interior to 0.160 AU (bottom panel) around each star, maintained their orbits for the duration of the integration.

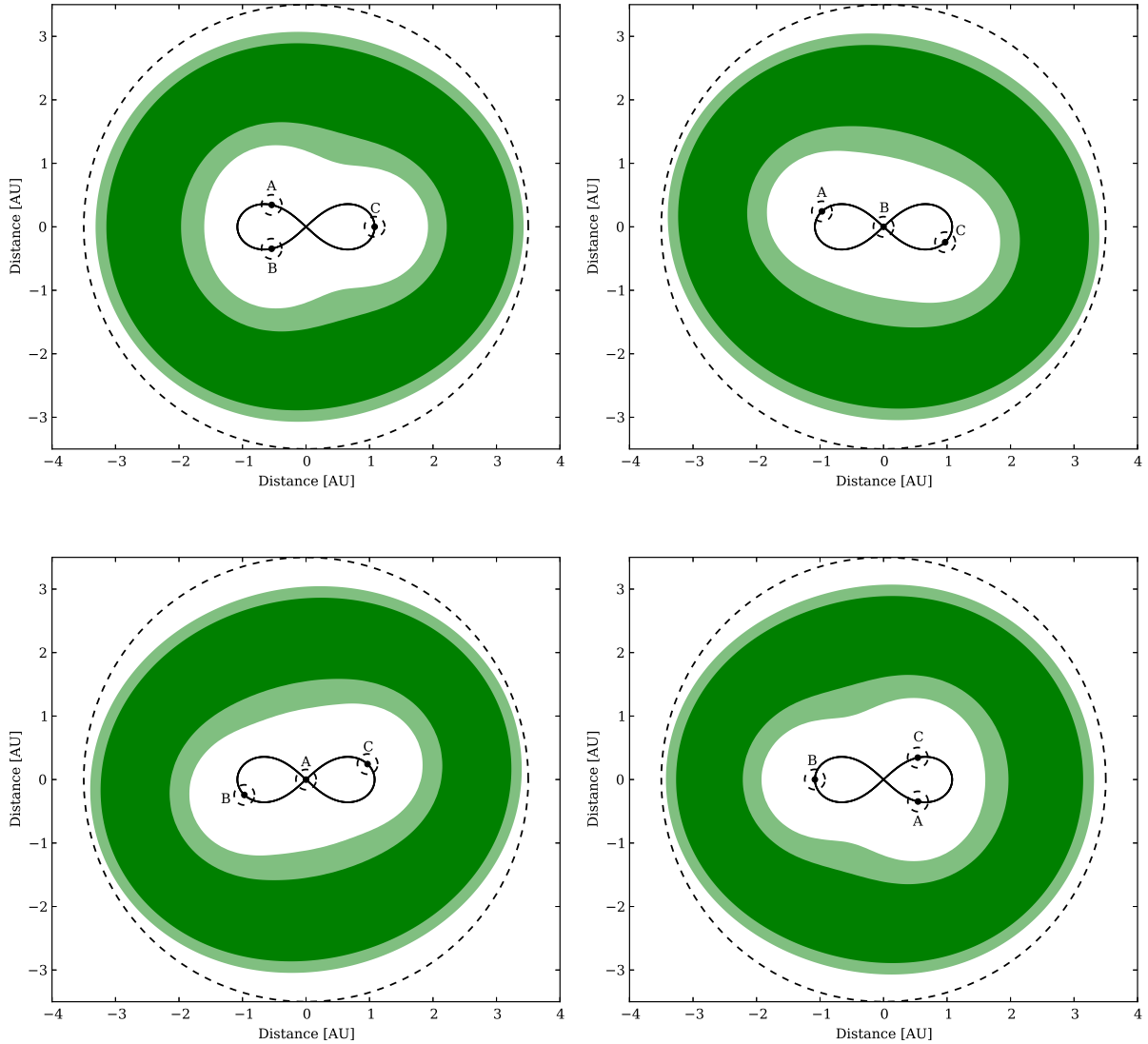


Fig. 14.— The HZ of a triple star system with Sun-like stars in a figure-eight orbit. From top-right panel, and in a counter-clockwise rotation, the figure show the evolution of the HZ of the system for one complete revolution around its center of mass. The initial orbital elements and velocities of the stars are given in Table 5. The dashed circles correspond to the boundaries of planetary orbit stability. As shown here, the HZ encompasses the entire system and is dynamically unstable. A movie of the HZ of this system can be found at <http://astro.twam.info/hz-multi>.

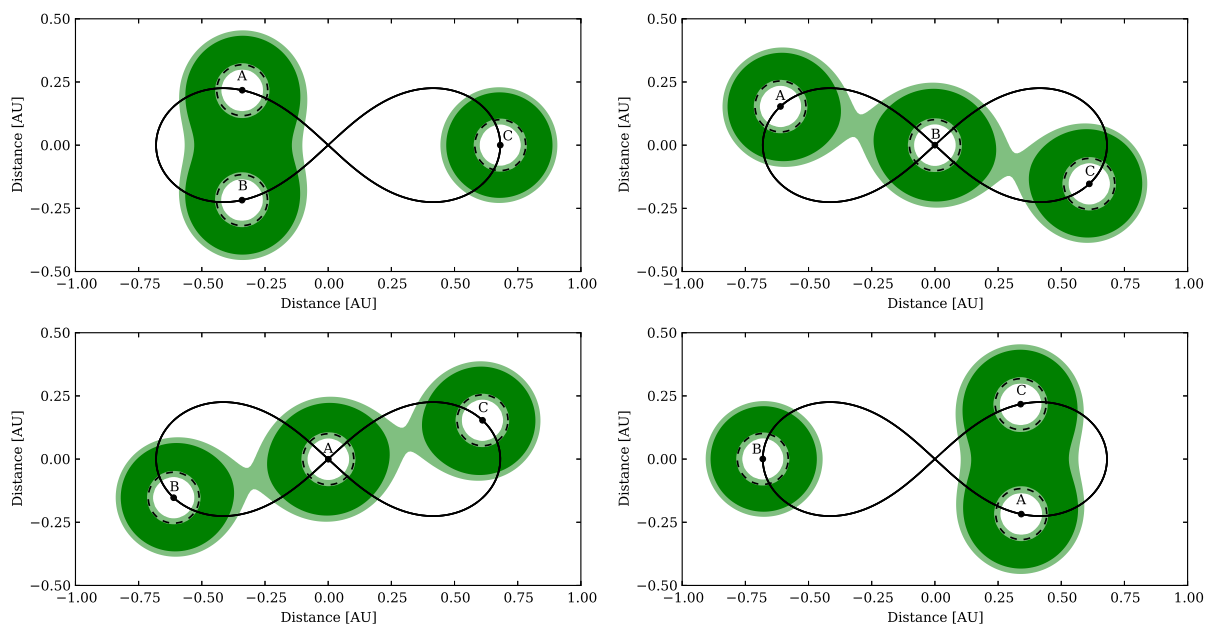


Fig. 15.— The HZ of a system of three 0.25 solar-mass M stars in a figure-eight orbit. From top-right panel and in a counter-clockwise rotation, the figure show the evolution of the HZ of the system for one complete revolution around its center of mass. The initial orbital elements and velocities of the stars are given in Table 5. The dashed circles show the boundaries of the regions of planetary stability around each star (~ 0.101 AU). As shown here, Earth-like planets can have stable orbits in a small region in the empirical HZ around each star. A movie of the HZ of this system can be found at <http://astro.twam.info/hz-multi>.

Table 1. Values of the coefficients of equation (2) from Kopparapu et al. (2013b)

	Narrow HZ		Empirical HZ	
	Runaway Greenhouse	Maximum Greenhouse	Recent Venus	Early Mars
F_{Sun}	1.06	0.36	1.78	0.32
d_{Sun} (AU)	0.97	1.67	0.75	1.77
a	1.2456×10^{-4}	5.9578×10^{-5}	1.4335×10^{-4}	5.4471×10^{-5}
b	1.4612×10^{-8}	1.6707×10^{-9}	3.3954×10^{-9}	1.5275×10^{-9}
c	-7.6345×10^{-12}	-3.0058×10^{-12}	-7.6364×10^{-12}	-2.1709×10^{-12}
d	-1.7511×10^{-15}	-5.1925×10^{-16}	-1.1950×10^{-15}	-3.8282×10^{-16}

Table 2. Values of the spectral weight factor

T (K)	2800	3500	4500	5500	5636	5780	6407	7400	8500
W_{in} (Narrow)	1.200	1.184	1.132	1.033	1.017	1.000	0.929	0.844	0.843
W_{out} (Narrow)	1.529	1.417	1.237	1.048	1.024	1.000	0.906	0.809	0.807
W_{in} (Empirical)	1.194	1.164	1.102	1.023	1.012	1.000	0.952	0.899	0.901
W_{out} (Empirical)	1.614	1.462	1.249	1.050	1.025	1.000	0.903	0.799	0.771

Table 3. The AB-C triplet in KID 5653126 system

Star	A	B	C
Mass (M_{\odot})	1.043	1.528	0.4
Luminosity (L_{\odot})	0.84	4.54	0.02
Temperature (K)	5636	6407	3561

Table 4. Values of the mass, luminosity, temperature, and the components of the position and velocity vectors of the equilateral three-star systems shown in Figures 11 and 12

	Circular			Elliptical		
	A	B	C	A	B	C
T (K)	3500	5500	7400	3500	5500	7400
L (L_{\odot})	0.028	0.063	6.6	0.028	0.063	6.6
M (M_{\odot})	0.4	0.5	1.6	0.4	0.5	1.6
a (AU)	5.32	5.13	2.19	2.96	2.85	1.21
e	0	0	0	0.8	0.8	0.8
X (AU)	3.64	-0.14	-3.64	3.36	-0.14	-3.64
Y (AU)	-3.88	2.18	-3.88	-3.88	2.18	-3.88
$V_X/2\pi$ (AU/day)	0.33	-0.19	0.33	0.13	-0.08	0.15
$V_Y/2\pi$ (AU/day)	0.29	-0.01	-0.31	0.14	-0.005	-0.13

Table 5. Values of the mass, luminosity, temperature, and the components of the position and velocity vectors of the three-star systems shown in Figures 14 and 15

	Sun-like stars			M stars		
	A	B	C	A	B	C
T (K)	5780	5780	5780	2800	2800	2800
L (L_{\odot})	1.0	1.0	1.0	0.0095	0.0095	0.0095
M (M_{\odot})	1.0	1.0	1.0	0.25	0.25	0.25
X (AU)	-0.97	0	0.97	-0.61	0	0.61
Y (AU)	0.24	0	-0.24	0.15	0	-0.15
$V_X/2\pi$ (AU/day)	0.47	-0.93	0.47	0.29	-0.59	0.29
$V_Y/2\pi$ (AU/day)	0.43	-0.86	0.43	0.27	-0.54	0.27